

Supplement of: *The Cretaceous physiological adaptation of angiosperms to a declining $p\text{CO}_2$: a modeling approach emulating paleo-traits*

Julia Bres¹, Pierre Sepulchre¹, Nicolas Viovy¹, and Nicolas Vuichard¹

¹Laboratoire des Sciences du Climat et de l'Environnement, LSCE/IPSL, CEA-CNRS-UVSQ, Université Paris-Saclay, 91191 Gif-sur-Yvette, France

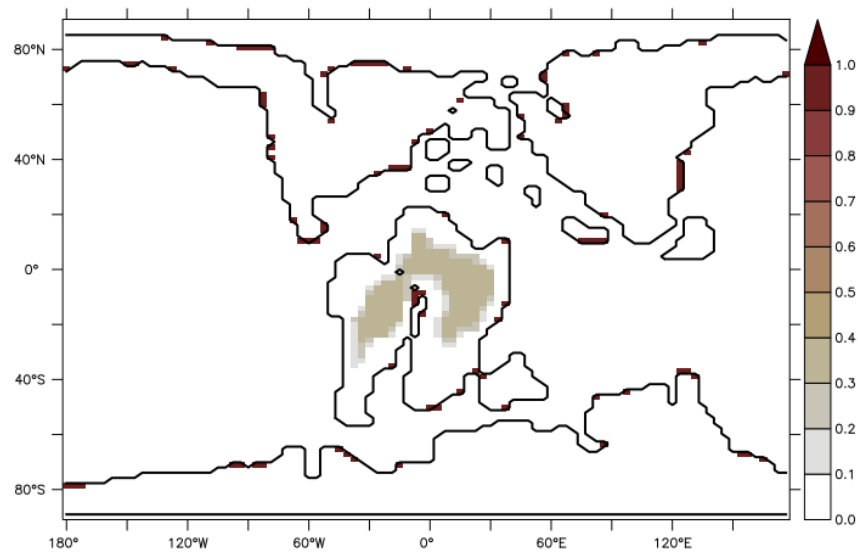
Correspondence: Julia Bres (julia.bres@lsce.ipsl.fr)

This supplement provides one additional table (**Table S1**) and several figures (from **Fig. S1** to **Fig. S10**). **Table S2** is given on a companion document.

. **Table S1** . Correspondence between biomes, inferred from paleobotanical data (Sewall et al., 2007), and PFTs: values are the percentage of surface of ground of grid-cell allocated to each PFT. The abbreviations are : High altitude/latitude, Evergreen, Conifer, closed canopy Forest (**HECF**); High altitude/latitude Mixed Forest with equal percentage of broad and needle leaved and evergreen and deciduous trees (**HMF**); High altitude/latitude, Moist, open canopy, Evergreen Forest with a shrub understory (**HMEF**); Low altitude/latitude, Evergreen, Conifer, closed canopy Forest (**LECF**); Low altitude/latitude, Moist, open canopy, Mixed evergreen/deciduous, Forest with a shrub understory (**LMMF**); closed canopy, Broad-leaved, Dry, Deciduous Forest (**BDDF**); savanna (dry, low understory with sparse, broad-leaved overstory) (**SAVA**); closed canopy, Broad-leaved, Moist, Evergreen Forest (**BMEF**); Wet or Cool Evergreen Shrubland (**WCES**); Dry or Warm Deciduous Shrubland (**DWDS**); Bare Soil (**BR**); Tropical Broad-leaved Evergreen (**TrBE**); Tropical Broad-leaved Raingreen (**TrBR**); Temperate Needleleaf Evergreen (**TeNE**); Temperate Broad-leaved Evergreen (**TeBE**); Temperate Broad-leaved summergreen (**TeBS**); Boreal Needleleaf Evergreen (**BoNE**); Boreal Broad-leaved Summergreen (**BoBS**); Boreal Needleleaf Summergreen (**BoNS**) and C3-grass (**NC3**).

	BR	TrBE	TrBR	TeNE	TeBE	TeBS	BoNE	BoBS	BoNS	NC3
HECF	0	0	0	100	0	0	0	0	0	0
HMF	0	0	0	50	0	50	0	0	0	0
HMEF	0	0	0	0	0	0	0	0	0	0
LECF	0	0	0	100	0	0	0	0	0	0
LMMF	0	35	35	0	0	0	0	0	0	30
BDDF	0	0	100	0	0	0	0	0	0	0
SAVA	0	0	10	0	0	0	0	0	0	90
BMEF	0	100	0	0	0	0	0	0	0	0
WCES	0	100	0	0	0	0	0	0	0	0
DWDS	30	0	30	0	0	0	0	0	0	40

The paleovegetation record mentions savannas composed of ferns (Coiffard et al., 2007) and “shrubby or herbaceous ‘savannah-like’ vegetation (without grasses)” (Bond and Scott, 2010). Because savannas are particularly hard to represent in DGVMs (Baudena et al., 2015), the savanna biome described by Sewall et al. (2007) as “dry, low understory with sparse broad leaved overstory” vegetation is represented by a combination of 90 % C3-grassland and 10 % of tropical broad-leaved evergreen (Table S1). This choice emulates a vegetation that is mostly of small height and that includes only little higher broad-leaved components, similar to the savanna description given by Sewall et al. (2007)).



. Figure S1 . Prescribed fraction of bare soil (unitless).

The prescribed fraction of bare soil (Fig. S1) corresponds to the fraction of grid-cell which is always bare soil over the 60 years of simulation.

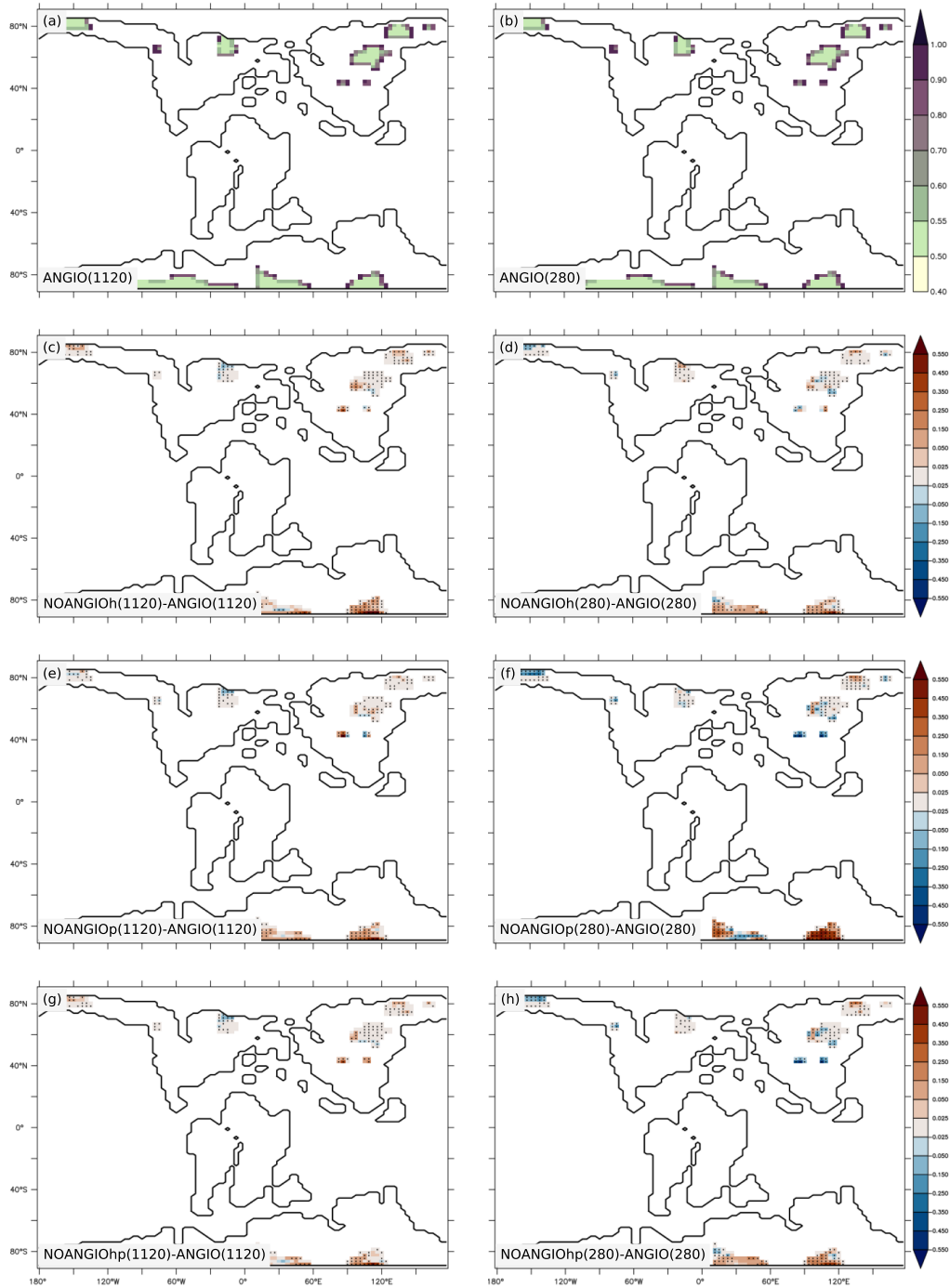


Figure S2 . Soil moisture stress for transpiration of gymnosperm (unitless) for (a) ANGIO(1120) and (b) ANGIO(280), anomalies of annual soil moisture stress for transpiration of gymnosperms (*10 - unitless) for (c) NOANGIOh(1120) vs ANGIO(1120), (d) NOANGIOh(280) vs ANGIO(280), (e) NOANGIOp(1120) vs ANGIO(1120), (f) NOANGIOp(280) vs ANGIO(280), (g) NOANGIOhp(1120) vs ANGIO(1120) and (h) NOANGIOhp(280) vs ANGIO(280). The t-test 95 % confidence level anomalies are given by dots.

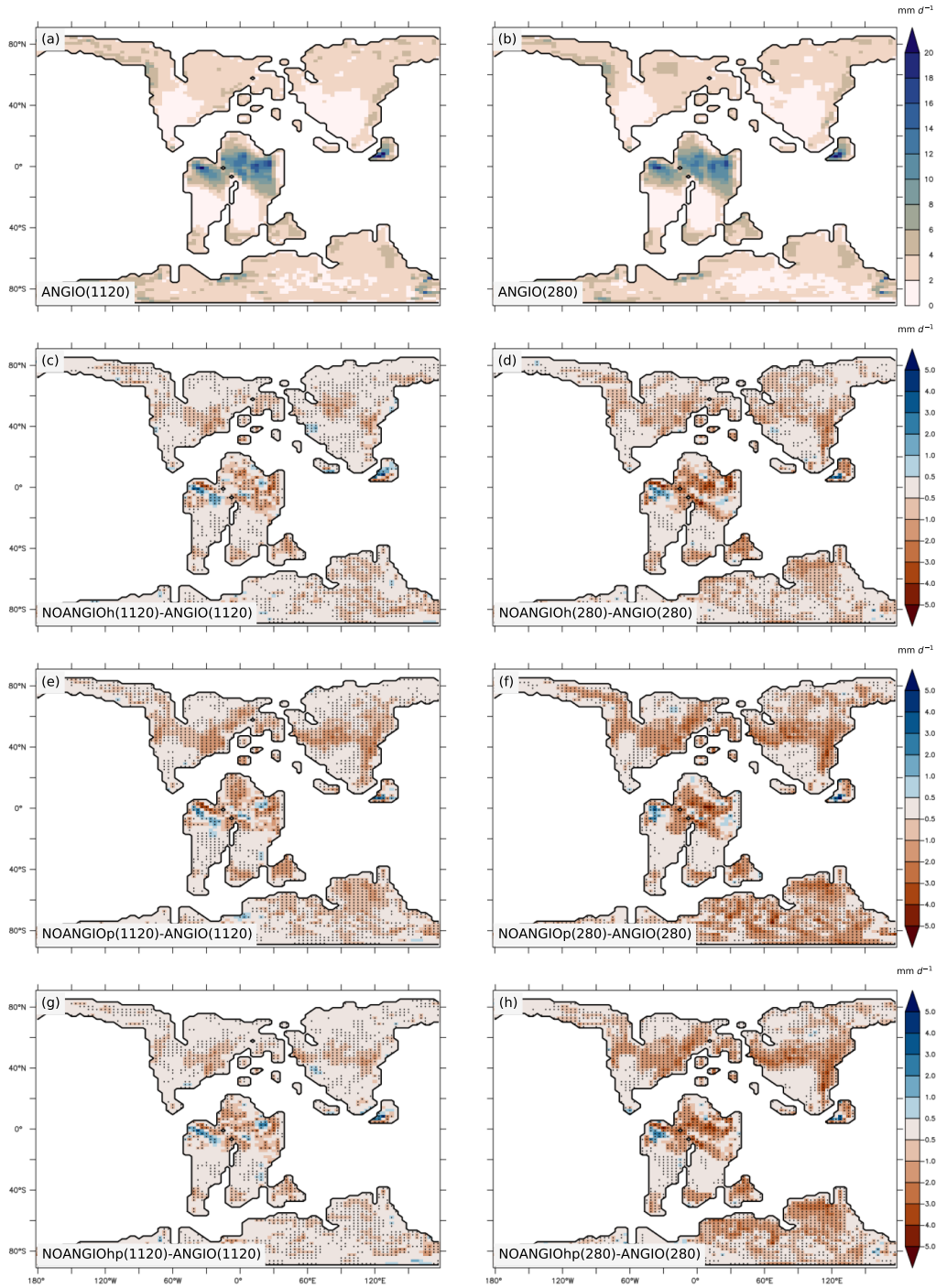


Figure S3 . Annual mean precipitation rates (mm d^{-1}) for (a) ANGIO(1120) and (b) ANGIO(280), anomalies of annual mean precipitation rates (mm d^{-1}) for (c) NOANGIOh(1120) vs ANGIO(1120), (d) NOANGIOh(280) vs ANGIO(280), (e) NOANGIOp(1120) vs ANGIO(1120), (f) NOANGIOp(280) vs ANGIO(280), (g) NOANGIOhp(1120) vs ANGIO(1120) and (h) NOANGIOhp(280) vs ANGIO(280). The t-test 95 % confidence level anomalies are given by dots.

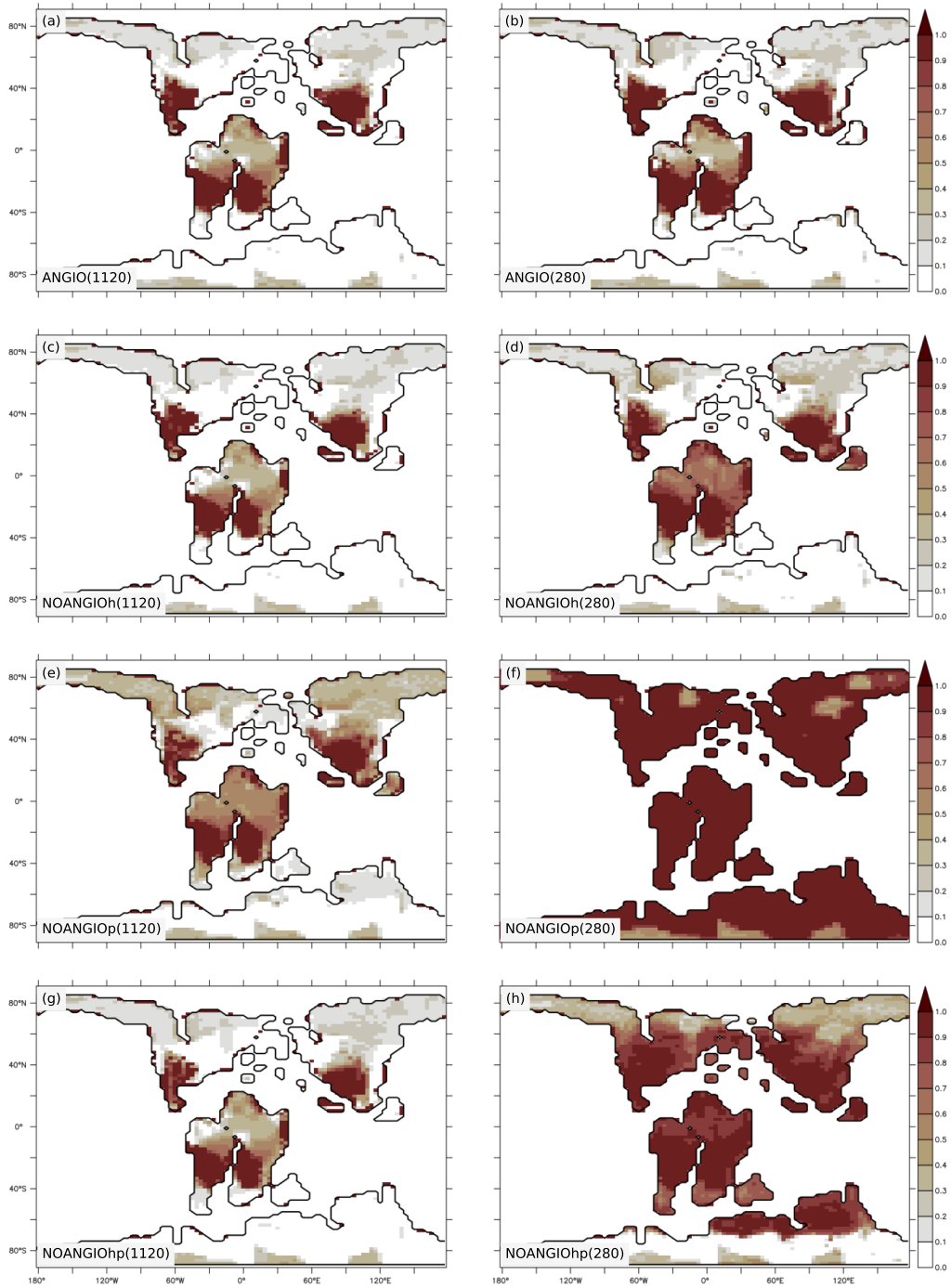


Figure S4 . Actual bare soil fraction (unitless) for a) ANGIO(1120), b) ANGIO(280), c) NOANGIOh(1120), d) NOANGIOh(280), e) NOANGIOp(1120), f) NOANGIOp(280), g) NOANGIOhp(1120) and h) NOANGIOhp(280). The fraction of actual bare soil is the annual mean.

Grid-cells where the vegetation collapses in the sensitivity experiments are replaced by bare soil, so as the actual bare soil fraction increases (i.e the actual surface that is not under vegetation, Fig. S4), and depends dynamically on the LAI.

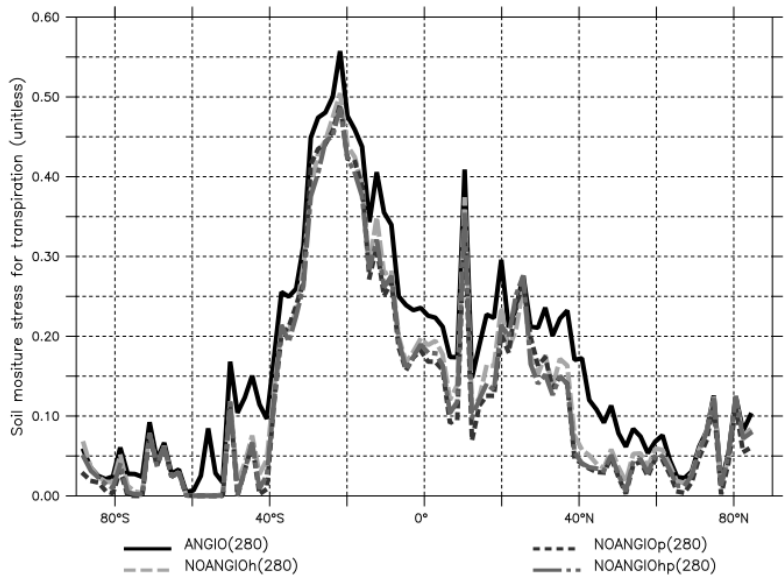


Figure S5a . Annual zonal mean of soil moisture stress for transpiration (unitless) for ANGIO(1120) (black line), NOANGIOh(1120) (light gray dashed line), NOANGIOp(1120) (dark gray dotted line) and NOANGIOhp(1120) (medium gray dashed/dotted line).

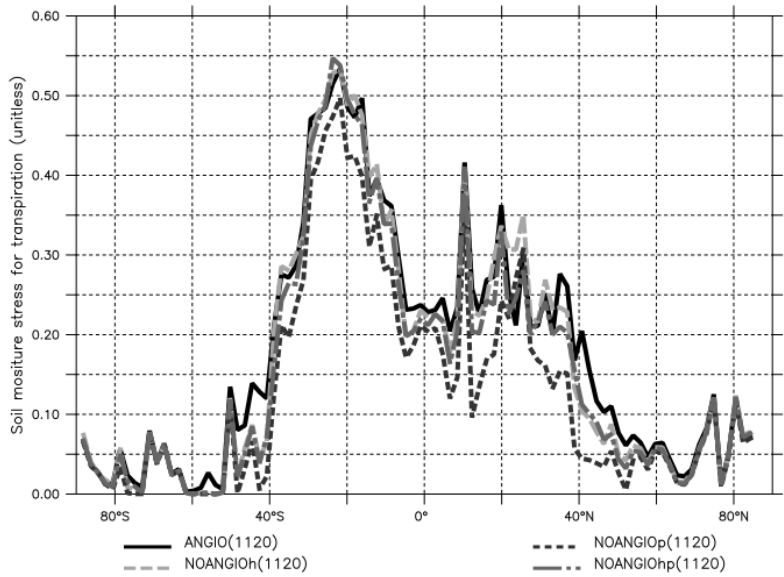


Figure S5b . Annual zonal mean of soil moisture stress for transpiration (unitless) for ANGIO(280) (black line), NOANGIOh(280) (light gray dashed line), NOANGIOp(280) (dark gray dotted line) and NOANGIOhp(280) (medium gray dashed/dotted line).

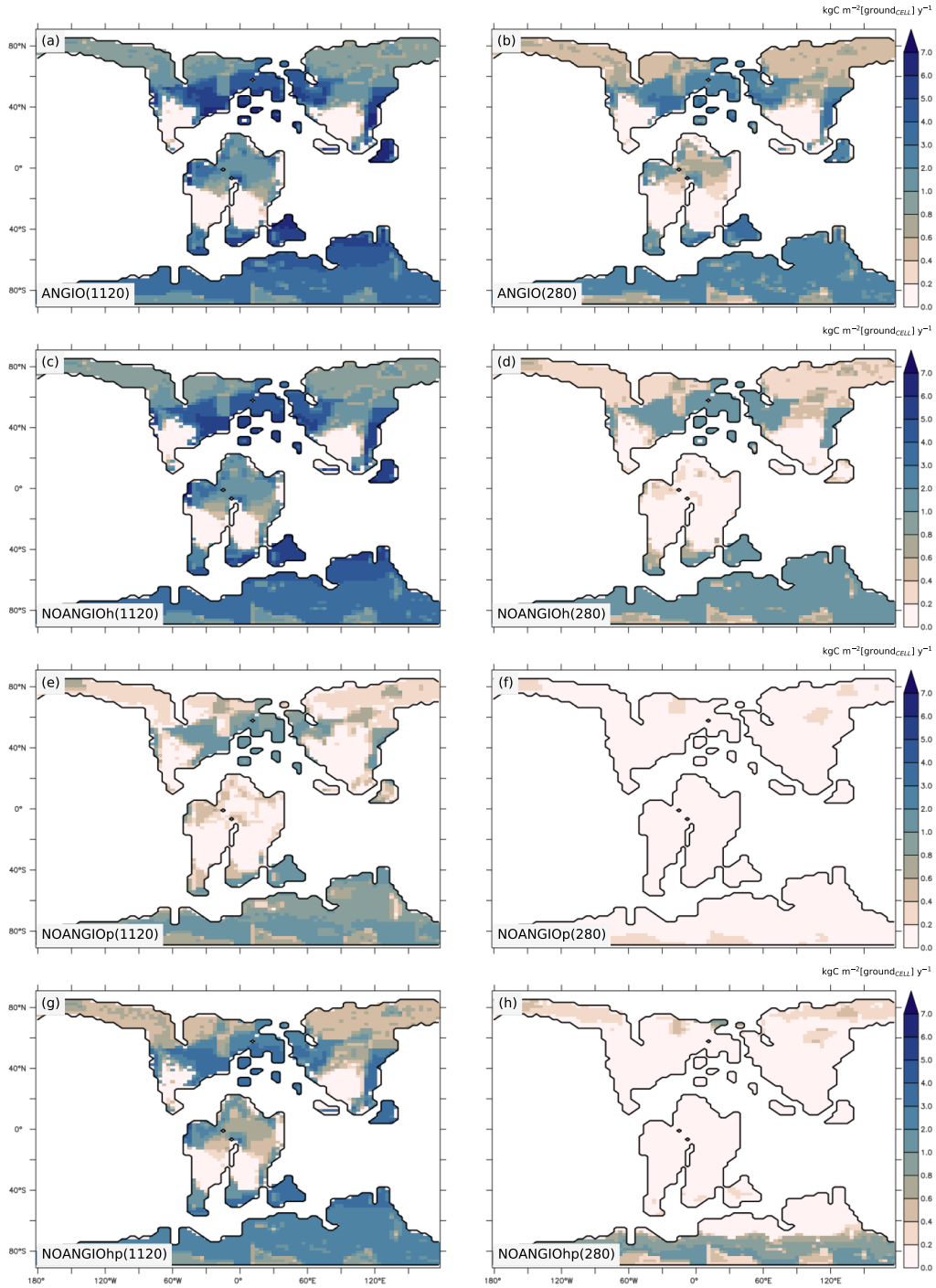


Figure S6 . Annual mean GPP ($\text{kgC m}^{-2}[\text{ground}_{\text{CELL}}] \text{ y}^{-1}$) for a) ANGIO(1120), b) ANGIO(280), c) NOANGIOh(1120), d) NOANGIOh(280), e) NOANGIOp(1120), f) NOANGIOp(280), g) NOANGIOhp(1120) and h) NOANGIOhp(280). The annual mean GPP is the weighted average of gross primary productivity of each PFT per surface of ground of a grid-cell (i.e. surface averaged across all PFTs including bare soil).

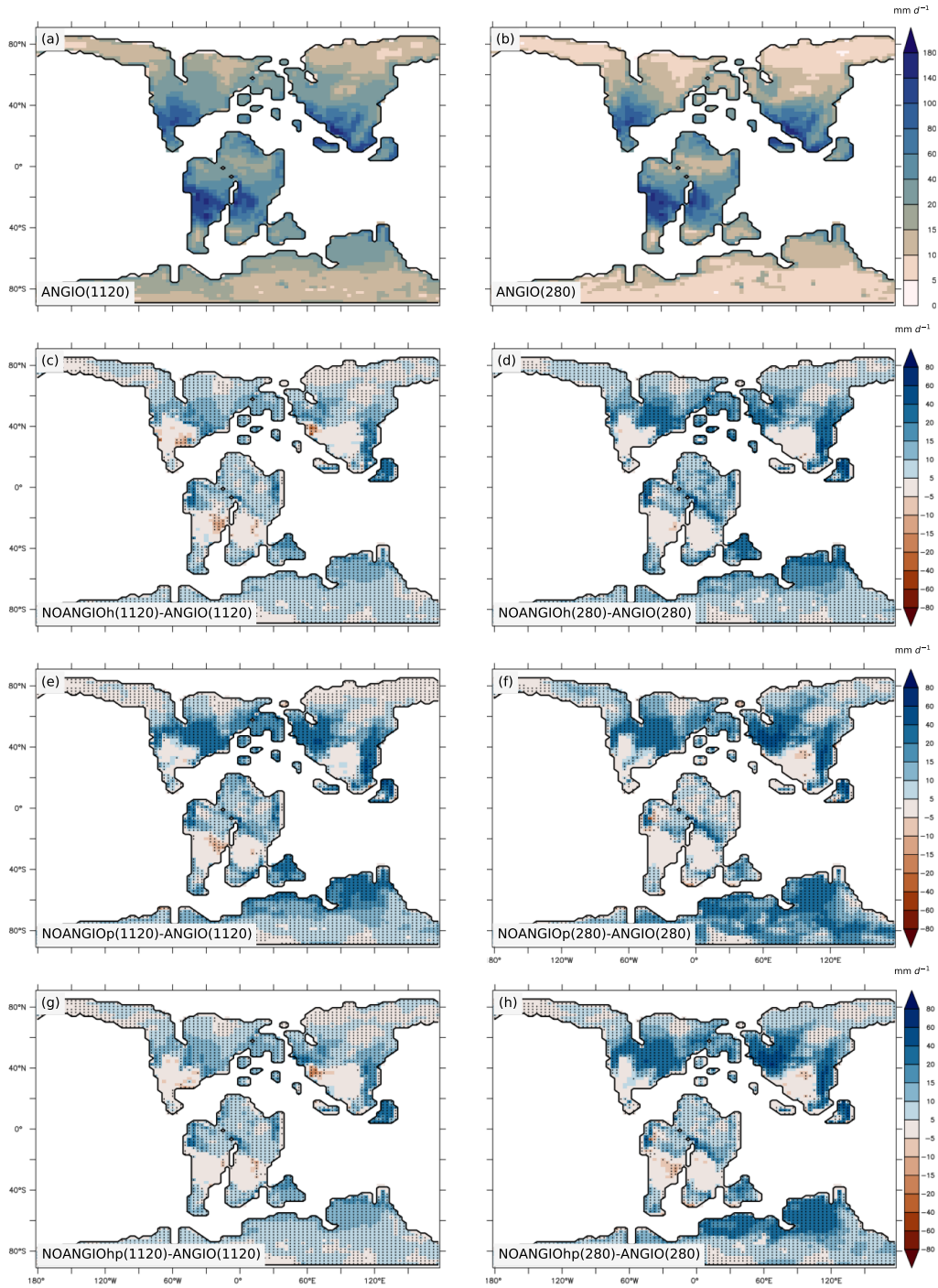


Figure S7 . Annual mean potential evaporation (mm d^{-1}) for a) ANGIO(1120) and b) ANGIO(280), anomalies of annual mean potential evaporation (mm d^{-1}) for c) NOANGIOh(1120) vs ANGIO(1120), d) NOANGIOh(280) vs ANGIO(280), e) NOANGIOp(1120) vs ANGIO(1120), f) NOANGIOp(280) vs ANGIO(280), g) NOANGIOhp(1120) vs ANGIO(1120) and h) NOANGIOhp(280) vs ANGIO(280). The t-test 95 % confidence level anomalies are given by dots.

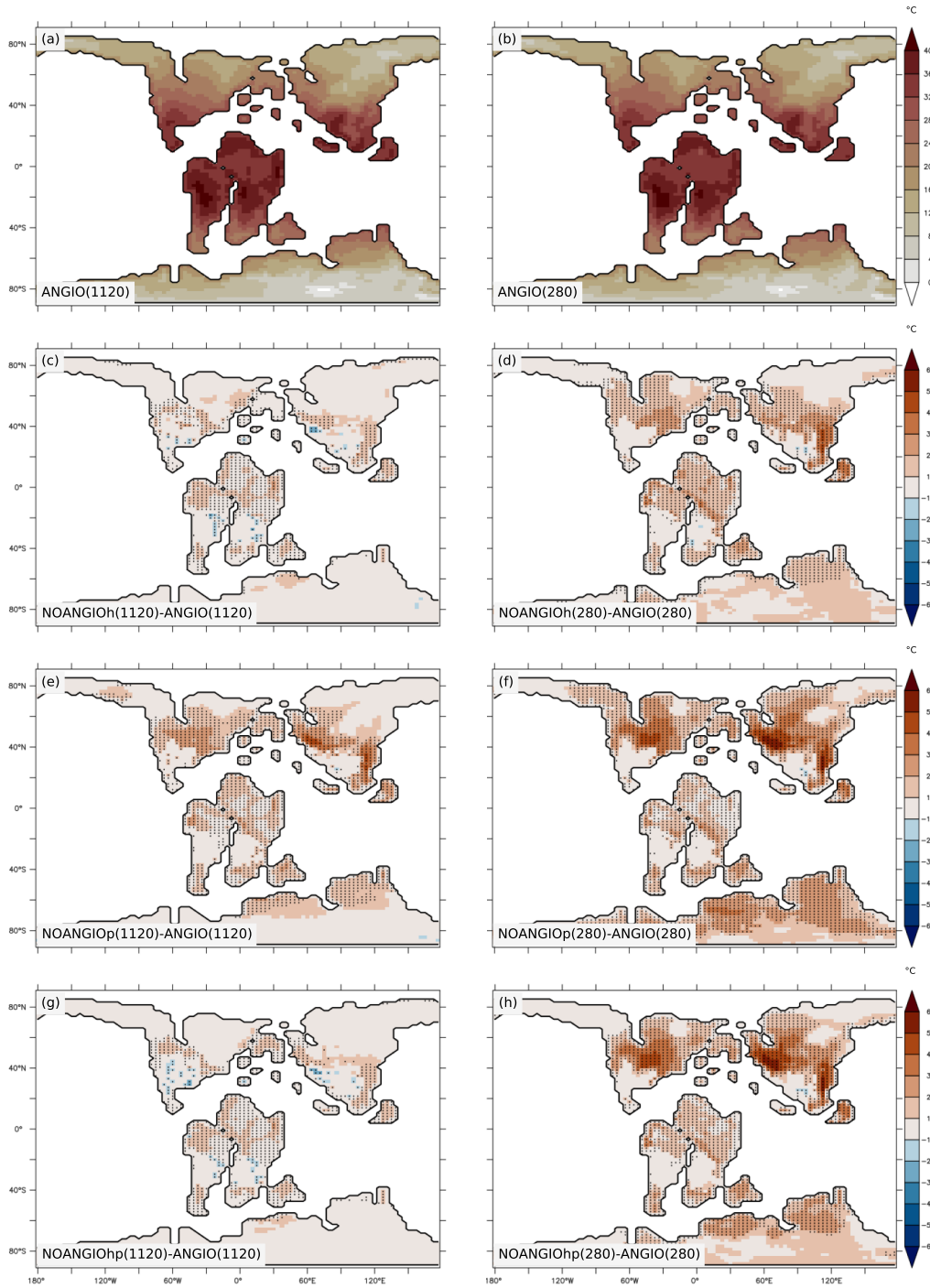


Figure S8 . Annual mean surface temperature (°C) for a) ANGIO(1120) and b) ANGIO(280), anomalies of annual mean surface temperature (°C) for c) NOANGIOh(1120) vs ANGIO(1120), d) NOANGIOh(280) vs ANGIO(280), e) NOANGIOp(1120) vs ANGIO(1120), f) NOANGIOp(280) vs ANGIO(280), g) NOANGIOhp(1120) vs ANGIO(1120) and h) NOANGIOhp(280) vs ANGIO(280). The t-test 95 % confidence level anomalies are given by dots.

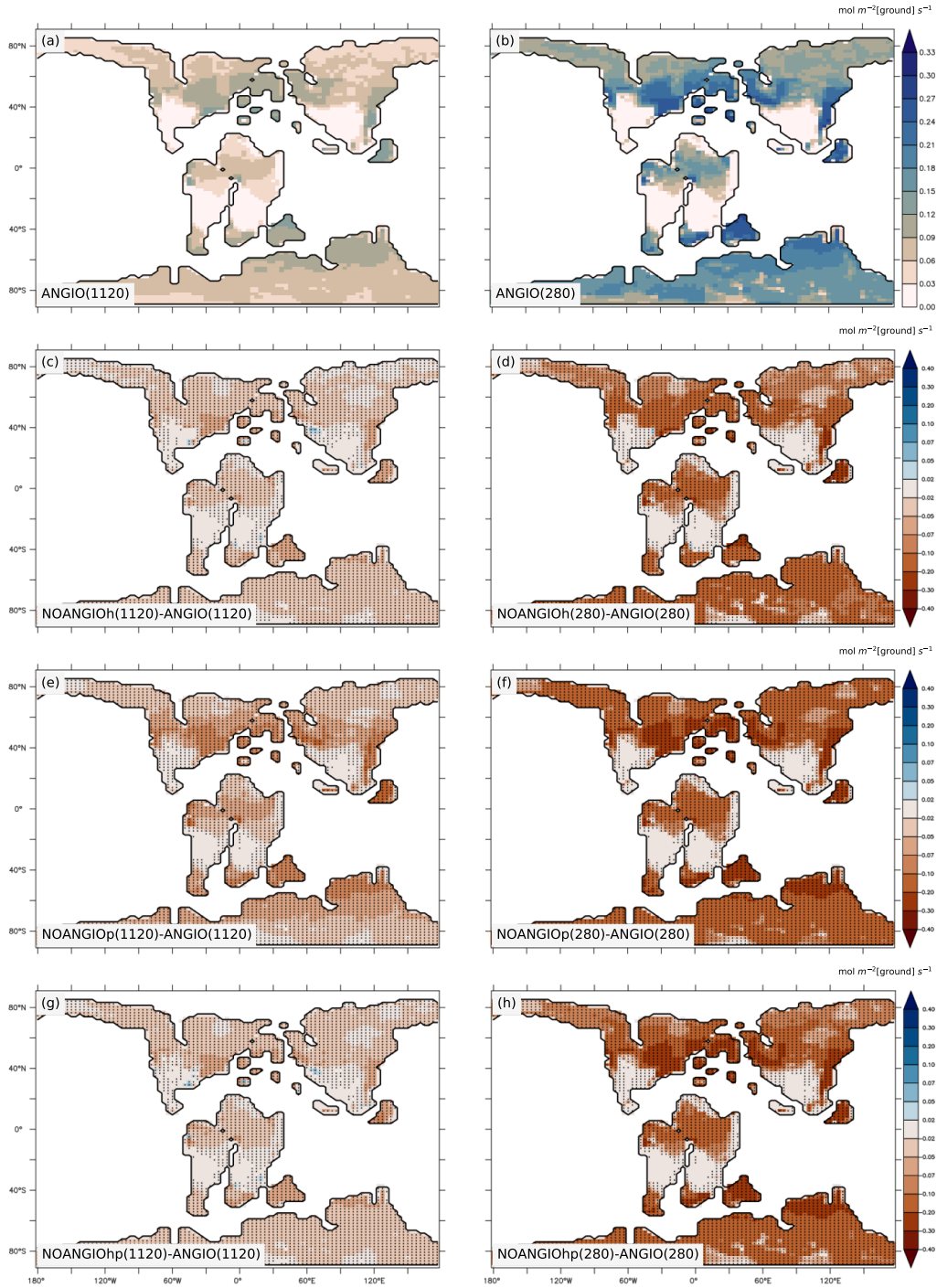


Figure S9 . Annual canopy stomatal conductance ($\text{mol m}^{-2}[\text{ground}_{CELL}] \text{ s}^{-1}$) for a) ANGIO(1120) and b) ANGIO(280), anomalies of annual mean canopy stomatal conductance ($\text{mol m}^{-2}[\text{ground}_{CELL}] \text{ s}^{-1}$) for c) NOANGIOh(1120) vs ANGIO(1120), d) NOANGIOh(280) vs ANGIO(280), e) NOANGIOp(1120) vs ANGIO(1120), f) NOANGIOp(280) vs ANGIO(280), g) NOANGIOhp(1120) vs ANGIO(1120) and h) NOANGIOhp(280) vs ANGIO(280). The t-test 95 % confidence level anomalies are given by dots.

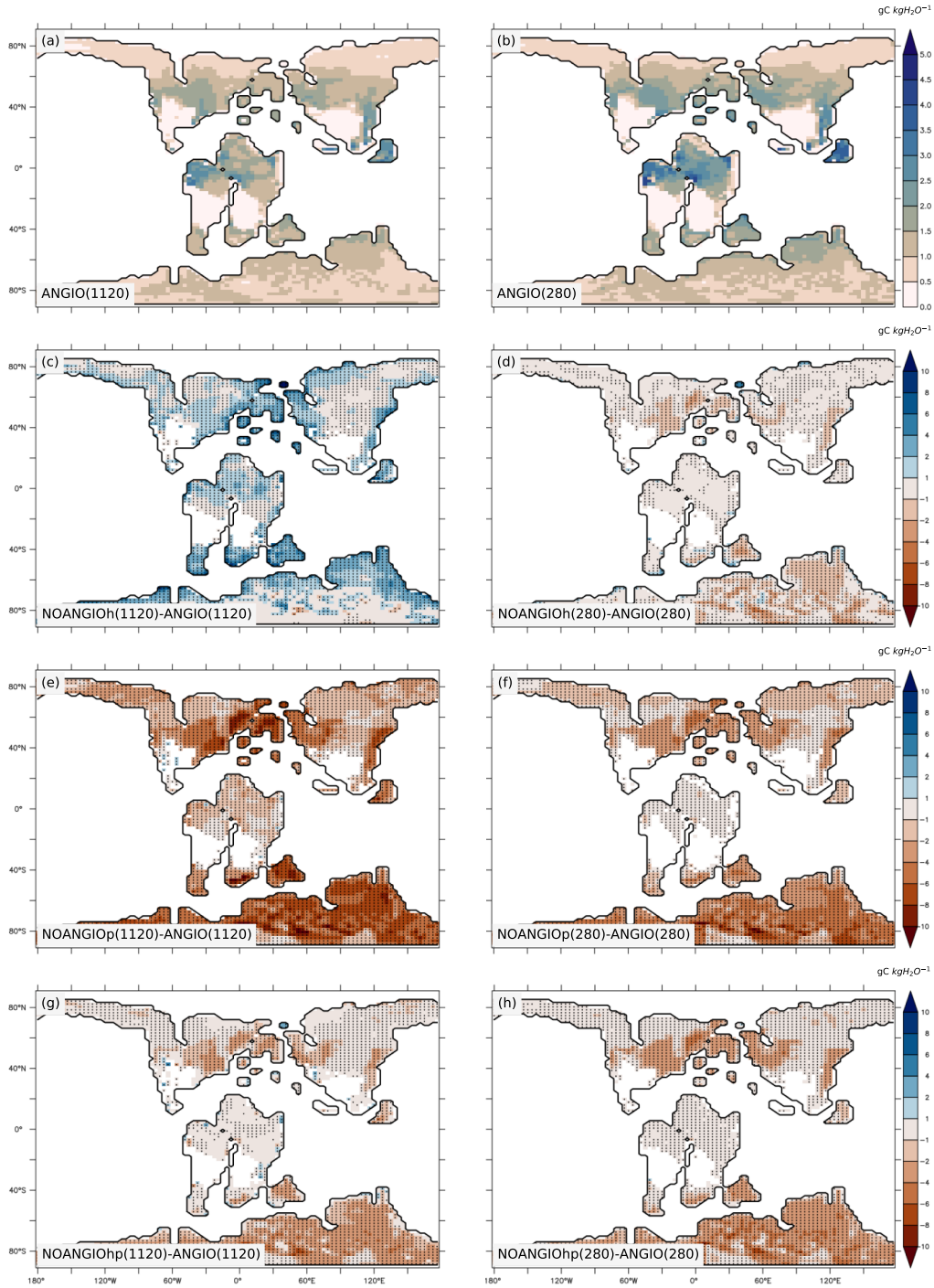


Figure S10 . Annual mean WUE ($\text{gC kgH}_2\text{O}^{-1}$) for a) ANGIO(1120), b) ANGIO(280), anomalies of annual mean WUE ($\text{gC kgH}_2\text{O}^{-1}$) for c) NOANGIOh(1120) vs ANGIO(1120), d) NOANGIOh(280) vs ANGIO(280), e) NOANGIOp(1120) vs ANGIO(1120), f) NOANGIOp(280) vs ANGIO(280), g) NOANGIOhp(1120) vs ANGIO(1120) and h) NOANGIOhp(280) vs ANGIO(280). The t-test 95 % confidence level anomalies are given by dots.

References

- Baudena, M., Dekker, S. C., van Bodegom, P. M., Cuesta, B., Higgins, S. I., Lehsten, V., Reick, C. H., Rietkerk, M., Scheiter, S., Yin, Z., et al.: Forests, savannas, and grasslands: bridging the knowledge gap between ecology and Dynamic Global Vegetation Models, *Biogeosciences*, 12, 1833–1848, <https://doi.org/10.5194/bg-12-1833-2015>, 2015.
- Bond, W. J. and Scott, A. C.: Fire and the spread of flowering plants in the Cretaceous, *New Phytologist*, 188, 1137–1150, <https://doi.org/https://doi.org/10.1111/j.1469-8137.2010.03418.x>, 2010.
- Coiffard, C., Gomez, B., and Thévenard, F.: Early Cretaceous angiosperm invasion of western Europe and major environmental changes, *Annals of Botany*, 100, 545–553, <https://doi.org/https://doi.org/10.1093/aob/mcm160>, 2007.
- Sewall, J. v., Van De Wal, R., Zwan, K. v., Oosterhout, C. v., Dijkstra, H., and Scotese, C.: Climate model boundary conditions for four Cretaceous time slices, *Clim. Past*, 3, 647–657, <https://doi.org/10.5194/cp-3-647-2007>, 2007.